ІНФОКОМУНІКАЦІЙНІ ТЕХНОЛОГІЇ ТА ЕЛЕКТРОННА ІНЖЕНЕРІЯ
INFORMATION AND COMMUNICATION TECHNOLOGIES, ELECTRONIC ENGINEERING

№ 4 (1), 2024

OPTIMIZATION OF THE PEROVSKITE SOLAR CELL STRUCTURE

N. Kuzyk [ORCID: 0009-0009-1293-2204], **S. Kutsiy** [ORCID: 0000-0002-0757-6059]

Lviv Polytechnic National University, 12, S. Bandery str., Lviv, 79013,Ukraine

Corresponding author: N. Kuzyk (e-mail: nataliia.i.kuzyk@lpnu.ua).

(Received 1 March 2024)

An experimental perovskite solar cell (PSC) with the structure Au/Spiro-MeOTAD/CH3NH3PbI3/PEDOT:PSS/ITO was fabricated. The measurements of main photovoltaic characteristics were provided. The current-voltage dependences (I-V curves) were measured conducted in the voltage range from -1V to 1V. During the measurements, the corresponding values were calculated of the short-circuit current density(Jsc) and open-circuit voltage(Uoc) were obtained as 1.23 mA/cm² and 0.19 V, respectively. Subsequently, an analytical model corresponding to this structure was formulated. For modeling the parameters of the perovskite solar cell, the Comsol Multiphysics environment was used, this environment is based on the finite element method. The relevant computations were provided to obtain the corresponding values of the short-circuit current density and open-circuit voltage as 3.29 mA/cm² and 0.2 V, respectively, with the maximum theoretically calculated power of this structure being 0.11 W. The experimental outcomes were juxtaposed with the predictions of the analytical computations, and the modeling results were empirically validated. An analytically accomplished model of the same structure was built by adding an electron transport layer (ETL). An organic material BCP (Bathocuproine) was used as an supplementary ETL layer. During the optimization of the PSC, the main datums were mathematically counted. Such values as the short-circuit current density of 10.17 mA/cm², open-circuit voltage of 1.2 V, and the maximum power value of Au/BCP/Spiro-MeOTAD/CH3NH3PbI3/PEDOT:PSS/ITO structure, which is 3.21 W were rated. A comparison of the volt-ampere characteristics of perovskite cells in dark and light modes was conducted for primary and optimized structures. The main parameters, obtained during the modeling of the experimental sample and subsequent model optimization, were compared. Specifically one of the key parameters of solar cell heterostructures the fill factor was evaluated and found to have increased from 16.52% to 25.00%, respectively. The light-sensitive behavior of the perovskite cell were visibly enhanced.

Keywords: *heterostructure, solar cells, perovskites, organic photovoltaic devices*
UDC: 53.072:53:004

1. Introduction

The utilization of organic photovoltaic technologies stands as a pivotal pursuit in advancing green energy [1]. Within this context, organic photovoltaic devices, characterized by high efficiency, cost-effectiveness, and scalability, garner substantial attention [2]. In the quest for superior and more economical alternative energy sources, perovskite solar cells (PSCs) occupy a prominent position [3]. Notably, the relatively elevated efficiency of PSCs, when compared to organic solar cells, renders them appealing for further investigation and practical implementation. Furthermore, the adaptability of

perovskite solar cells to flexible substrates, coupled with their low-cost production technology, underscores their potential [4, 5]

Characteristic parameters of photoactive perovskites, which make them promising materials for solar energy, include properties such as a high coefficient of optical absorption (~10^5 cm^{-1}), a low exciton binding energy (~20 meV), and a relatively large charge carrier free path length (~1 μm), as well as the ability to operate solar cells based on this material at low temperatures [3, 6, 7].

Over the past decade, there has been a true breakthrough in the technology of manufacturing organic solar cells based on perovskites, characterized by an increase in the fill factor from 3.8% efficiency of energy conversion to the certified record efficiency of perovskite solar cells, which is 25.5% [3]. Good results have been achieved due to the introduction of new technologies for chemical processing and effective modified approaches to the deposition of functional films and heterostructures based on them. Based on these methods, uniform and highly crystalline perovskite films have been developed and fabricated, which increase the efficiency of organic photovoltaic devices. In this context, the introduction of materials with a broad spectrum of photosensitivity and perfect structure into the technology of manufacturing PSCs, such as methylammonium lead triiodide (MAPbI3, CH3NH3PbI3), is also promising, allowing for high efficiency and improved stability [8, 9, 10]. Despite rapid progress, the efficiency of perovskite solar cells is still far from their theoretical limits. The key factor for further increasing the efficiency of perovskite solar cells is the optimization of the architecture of high-quality PSCs to reduce non-radiative recombination in perovskite active layers and minimize interface defects in structural layers [8, 9, 11, 12].

The operation of solar cells based on heterostructures can proceed without the involvement of electron transport layers (ETL) and hole transport layers (HTL) in the photovoltaic conversion process, as demonstrated in early investigations of solar cells [4, 11]. The inclusion of hole transport layers (HTL) and electron transport layers (ETL) in efficient perovskite solar cells (PSCs) plays a critical role in electron collection and their subsequent transport from the absorber layer to the corresponding electrodes [4, 12]. Imbalance in the operation of transport layers results in differences in drift currents of charge carriers to the respective electrodes and significantly affects the device performance. Additionally, the absence or presence of inefficient transport layers increases the device's resistance, thereby contributing to a decrease in the fill factor of the solar cell. Consequently, judiciously selecting and optimizing the layers within perovskite solar cells assumes paramount importance in achieving maximal device efficiency [11].

Hence, ongoing endeavors focus on formulating analytical models to fabricate organic solar cells featuring a multilayer architecture, including perovskite solar cells [13]. Theoretical modeling of sophisticated solar cell designs facilitates more effective material selection and application.

In this investigation, we perform experimental assessments and develop a mathematical model to analyze the optical properties of the Au/Spiro-MeOTAD/$CH_3NH_3PbI_3$/PEDOT: PSS/ITO architecture. Our objective is to enhance the light-sensitive behavior of the perovskite cell. The analytical model is subsequently validated to refine the design of photogenerating devices. Specifically, we optimize the structure of the perovskite-based solar cell by incorporating an electron transport layer (ETL) [11].

2. Materials and experimental procedures

The experimental structure of the photosensitive element was formed on the surface of a glass plate with a deposited layer of ITO [Indium Tin Oxide]. The optically transparent conductive layer of ITO was pretreated with ozone plasma before applying the PEDOT:PSS film. This technological operation improves the adhesion of the hole-injection layer of PEDOT:PSS and enables enhancement of the conductivity and work function of the PEDOT:PSS film [14,15].

The PEDOT:PSS film was formed from an aqueous solution using the spin-coating method, followed by thermal annealing in an inert atmosphere in a nitrogen glove box [Laboratory Glove Box

L2007A1-UK] at 50°C for 15 minutes. The thickness of the PEDOT:PSS film was controlled by measurement using a profilometer and 3D optical profiler, with a working thickness of 50 nm.

After applying the perovskite pigment film [Perovskite Precursor Ink for Air Processing], a thermal treatment process was conducted for 60 minutes at 100°C with humidity control.

The next technological operation was the application of a Spiro-OMeTAD film [Spiro-OMeTAD] (dj=300 nm) using the spin-coating method. To improve the optical properties of Spiro-OMeTAD [16], the sample was left in the air for 12 hours. An electrically conductive gold film with a thickness of 80 nm was deposited on the surface of the formed heterostructure using thermal evaporation at a residual pressure of 10^{-5} Torr. The zone diagram of the experimental photosensitive structure and a photograph of the fabricated device are presented in Fig. 1.

The experimentally fabricated sample of the perovskite cell was tested using a parametric semiconductor analyzer [4145A SEMICONDUCTOR PARAMETER ANALYZER HEWLETT PACKARD] in dark mode and under illumination with a solar light simulator.

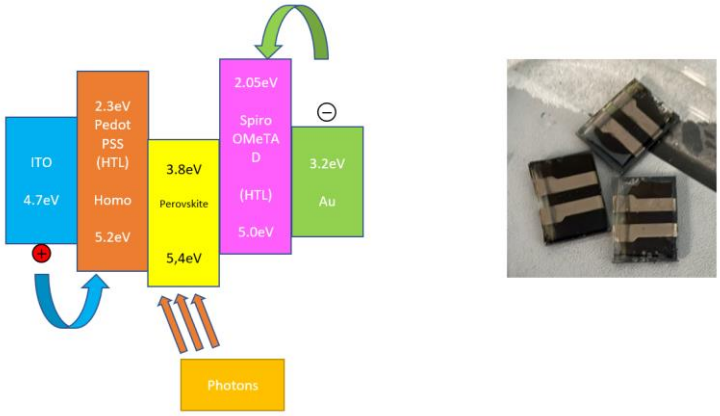

a *b*

Fig. 1. The energy band structure (a) and the photograph of the experimental sample of a perovskite solar cell Au/Spiro-MeOTAD/CH3NH3PbI3/PEDOT:PSS/ITO structure Solar irradiation spectrum for AM0 and AM1.5 illumination.

The experimentally fabricated sample of the perovskite cell was tested using a parametric semiconductor analyzer [4145A SEMICONDUCTOR PARAMETER ANALYZER HEWLETT PACKARD] in dark mode and under illumination with a solar light simulator (100 mW/cm²), the spectrum of which is presented in Fig. 2.

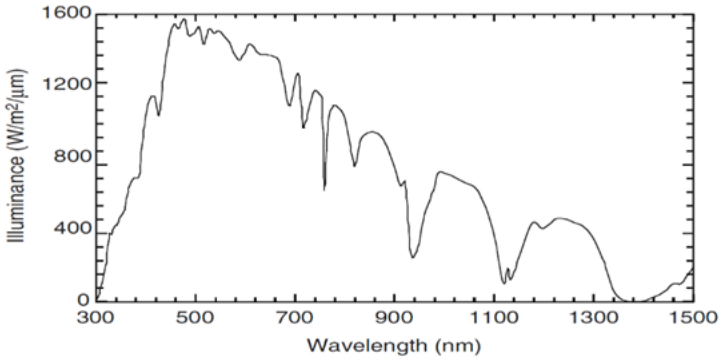

Fig. 2. Solar irradiation spectrum for AM0 and AM1.5 illumination.

The measurements of the current-voltage characteristics (I-V curves) were conducted in the voltage range from -1V to 1V. During the measurements, the corresponding values of the short-circuit current density and open-circuit voltage were obtained as 1.23 mA/cm² and 0.19 V, respectively, yielding a fill factor value of ff=19%. The IV curve of the experimental sample under different operating conditions is

depicted in Fig. 3. The device's power conversion efficiency was determined as the ratio of the maximum power (P_m) under no load to the power of the incident light P_0 .

$$\eta_e = P_m / P_0 \tag{1}$$

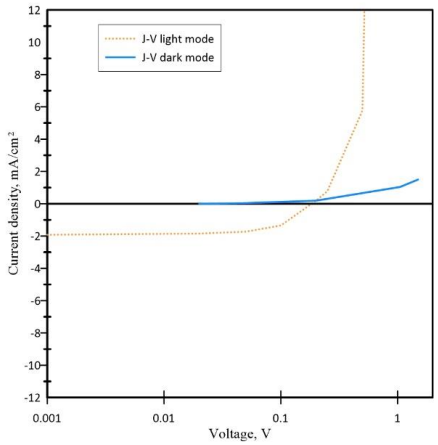

Fig. 3. Dark and light mode current-voltage characteristics of the experimentally developed perovskite cell sample with the structure Au/Spiro-MeOTAD/CH3NH3PbI3/PEDOT:PSS/ITO

Table 1 presents the experimental parameters of the perovskite solar cells (PSCs)

Table 1.

Experimental parameters of the structure Au/Spiro-MeOTAD/CH3NH3PbI3/PEDOT:PSS/ITO

I_m (current at maximum power)	10.3	мА
U_m (voltage at maximum power)	0.42	В
I_{sc} (short-circuit current)	1.23	мА
U_{oc} (open-circuit voltage)	0.19	В
ff (fill factor)	18.51	%
η (power conversion efficiency)	4.32	%

3. Modeling and optimization

For modeling the parameters of the perovskite solar cell, the Comsol Multiphysics environment was utilized, based on the finite element method. In the course of the calculations, the Poisson's equation (2) was employed to describe the physical process, linking the electrostatic potential with the total charge density, along with the continuity equations for holes and electrons (3) and (4). Additionally, statistical effects of Shockley-Read-Hall recombination were considered.

$$\frac{d^2}{dx^2}\Phi(x) = \frac{q}{\varepsilon\varepsilon_0}\left(p(x) - n(x) + N_D + N_A + n_t^+ + n_t^-\right) \tag{2}$$

$$-\left(\frac{1}{q}\right)\frac{\partial J_p}{\partial x} - U_p + G = \frac{\partial p}{\partial t} \tag{3}$$

$$\left(\frac{1}{q}\right)\frac{\partial J_n}{\partial x} - U_n + G = \frac{\partial n}{\partial t} \tag{4}$$

In equation (1), the symbol Φ represents the electrostatic potential, q is the electron charge, ε_r and ε_0 indicate the relative dielectric permittivity and electric constant, respectively, p and n represent the

concentrations of holes and electrons, N_D and N_A are the concentrations of donor and acceptor impurities, and n_t^+ and n_t^- are the concentrations of traps for holes and electrons, respectively. In equations (2) and (3), J_n and J_p denote the densities of electric current for electrons and holes.

The equations describing the movement of anions (a^-) and cations (c^+), taking into account the drift-diffusion equations (5-6) [20]

$$-\left|\left(\frac{1}{q}\right)\right|\frac{\partial J_{c^+}}{\partial x}=\frac{\partial c}{\partial t} \tag{5}$$

$$\frac{1}{q}\frac{\partial J_{a^-}}{\partial x}=\frac{\partial a}{\partial t} \tag{6}$$

Taking into account the concentrations of anions (a^-) and cations (c^+) in the Poisson's equation, we obtain:

$$\frac{d^2}{dx^2}\Phi(x)=\frac{q}{\varepsilon\varepsilon_0}\left(p(x)-n(x)+N_D+N_A+n_t^++n_t^-+\left(c^+-a^-\right)\right) \tag{7}$$

The neutral state for perovskite is satisfied by the equation:

$$\frac{1}{l}\iint a^-(x)dx=\frac{1}{l}\iint c^+(x)dx=N_i\,, \tag{8}$$

where l is the thickness of the perovskite layer, and N_i is the ion density.

At the interfaces of the perovskite with the electron and hole transport layers, charge carriers have the property of tunneling into the ETL and HTL layers. To account for this tunneling effect, an approximation was applied.

The boundary condition of the modeling problem for ion transport was the absence of ion flux in the ETL and HTL layers, which is satisfied by the equations:

$$n.J_a=0\,, \tag{9}$$

$$n.J_c=0\,, \tag{10}$$

$$J_a=q\mu_a aE+qD_a\frac{\partial a}{\partial x}\,, \tag{11}$$

$$J_c=q\mu_c cE+qD_c\frac{\partial c}{\partial x}\,, \tag{12}$$

Where the current densities of anions J_a and cations J_c, and their respective diffusion coefficients D_a and D_c are taken into account. For the initial analytical model, the structure shown in Figure 4 was applied. The parameters of the Spiro-MeOTAD and PEDOT:PSS materials were modeled using [11] and [12], respectively, and are provided in Table 2. All other material parameters were taken from the Comsol library. Based on this model, an analytical model with an additional ETL layer was proposed and modeled (Figure 4). The presence of an ETL layer in effective PSCs is important for electron collection and transport from the absorber to the respective electrodes. However, the use of an ETL layer in PSCs increases the electron-hole recombination resistance due to a slight increase in series resistance (R_s).

Balanced selection and optimization of layers in perovskite solar cells are important for achieving optimal performance, which includes considering recombination resistance and series resistance to maximize device efficiency [19].

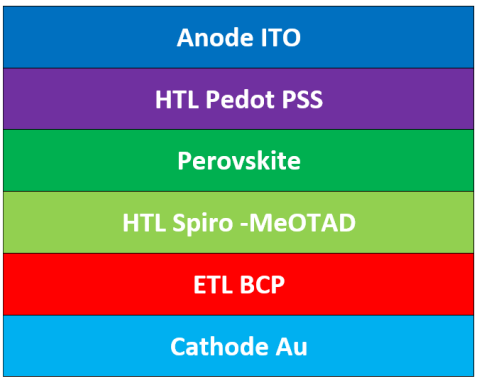

Fig. 4. Layer-by-layer structure of the optimized perovskite cell Au/BCP/Spiro-MeOTAD/CH3NH3PbI3/PEDOT:PSS/ITO

An organic material BCP (Bathocuproine) was used as an additional ETL layer, which is often employed in the production of organic PSCs and other electronic devices. BCP possesses high electron conductivity and is well-suited for forming thin films on the surfaces of other materials [18, 21]. The use of BCP can improve the efficiency and stability of PSCs and other electronic devices [19]. Table 2 lists the main parameters applied in the modeling process.

Table 2.

Main parameters applied in the modeling process

Parameters and dimensions	**BCP**	**Spiro-MeOTAD**	**Perovskite CH3NH3PbI3**	**PEDOT:PSS**
Layer thickness, nm	50	300	300	50
Relative permittivity $\varepsilon_0\varepsilon$	31	3	35	3
Band gap, E_{g0}, eV	3,5	2,95	1,6	2,2
Electron affinity, χ_0, eV	4,1	6,74	5	5
Effective density of states, valence band, N_v, 1/cm^3	$1*10^{20}$	$8,67*10^{14}$	$5*10^{25}$	$1*10^{20}$
Effective density of states, conduction band, N_c, 1/cm^3	$1*10^{20}$	$8,67*10^{14}$	$5*10^{25}$	$1*10^{20}$
Electron mobility, μ_n, cm^2/V×s	$1*10^{-2}$	$2*10^{-4}$	4.8	$1*10^{-2}$
Hole mobility, μ_p, cm^2/V×s	$5*10^{-2}$	$2*10^{-4}$	4.8	$5*10^{-2}$
Electron lifetime, ns	5	5	5	5

4. Main modeling results and conclusions

In the Comsol Multiphysics software, the current-voltage characteristics of the Au/Spiro-MeOTAD/CH3NH3PbI3/PEDOT:PSS/ITO structure were mathematically modeled in both dark and light modes, as depicted in Figure 5. During the calculations, the corresponding values of the short-circuit current density and open-circuit voltage were obtained as 3.29 mA/cm² and 0.2 V, respectively, with the maximum theoretically calculated power of this structure being 0.11 W. Using formula (1), the fill factor value was calculated to be 16.52%. Modeled and experimental data exhibit some discrepancies, which can be attributed to errors in measuring layer thicknesses, morphological parameters of the layers, and surface defects.

The current density - voltage curve for the Au/BCP/Spiro-MeOTAD/CH3NH3PbI3/PEDOT:PSS/ITO structure and optimized J-V curve with an additional electron

transport layer, is shown in Figure 5. During the optimization of the perovskite cell, the main parameters were mathematically calculated, such as the short-circuit current density of 10.17 mA/cm², open-circuit voltage of 1.2 V, and the maximum power value of this structure, which is 3.21 W. Based on all the parameters mentioned above, the fill factor (1)was calculated to be 25.00%.

As observed, the optimization of the photosensitive device through the addition of an electron transport layer led to a significant improvement in the efficiency of the solar cell.

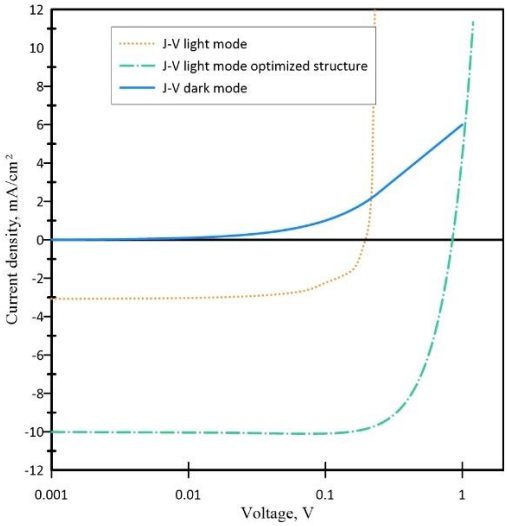

Fig. 5. Current-voltage characteristics of the modeled experimental sample with the structure Au/Spiro-MeOTAD/CH3NH3PbI3/PEDOT:PSS/ITO and the optimized structure Au/BCP/Spiro-MeOTAD/CH3NH3PbI3/PEDOT:PSS/ITO

Acknowledgment

This work was approved and supported by the Ministry of Education and Science of Ukraine (Project DB/Infra state registration number 0123U101690)

References

[1]. Nayak, P. K., Mahesh, S., Snaith, H. J., & Cahen, D. (2019). Photovoltaic solar cell technologies: analysing the state of the art. Nature Reviews Materials, 4(4), 269-285.

[2]. Tao, Q., Xu, P., Li, M., & Lu, W. (2021). Machine learning for perovskite materials design and discovery. npj Computational Materials, 7(1), 23.

[3]. Zhang, L., Mei, L., Wang, K., Lv, Y., Zhang, S., Lian, Y., ... & Ding, L. (2023). Advances in the application of perovskite materials. Nano-Micro Letters, 15(1), 177.

[4]. Rai, N., Rai, S., Singh, P. K., Lohia, P., & Dwivedi, D. K. (2020). Analysis of various ETL materials for an efficient perovskite solar cell by numerical simulation. Journal of Materials Science: Materials in Electronics, 31, 16269-16280.

[5]. Al-Shahri, O. A., Ismail, F. B., Hannan, M. A., Lipu, M. H., Al-Shetwi, A. Q., Begum, R. A., ... & Soujeri, E. (2021). Solar photovoltaic energy optimization methods, challenges and issues: A comprehensive review. Journal of Cleaner Production, 284, 125465

[6]. , Kong, J., Wang, H., Rohr, J. A., Fishman, Z. S., Zhou, Y., Li, M., ... & Taylor, A. D. (2020). Perovskite solar cells with enhanced fill factors using polymer-capped solvent annealing. ACS Applied Energy Materials, 3(8), 7231-7238.

[7]. Chen, Y., Tan, S., Li, N., Huang, B., Niu, X., Li, L., ... & Zhou, H. (2020). Self-elimination of intrinsic defects improves the low-temperature performance of perovskite photovoltaics. Joule, 4(9), 1961-1976.

[8]. Kong, J., Wang, H., Rohr, J. A., Fishman, Z. S., Zhou, Y., Li, M., ... & Taylor, A. D. (2020). Perovskite solar cells with enhanced fill factors using polymer-capped solvent annealing. ACS Applied Energy Materials, 3(8), 7231-7238.

[9]. Hossain, M. K., Toki, G. I., Kuddus, A., Rubel, M. H. K., Hossain, M. M., Bencherif, H., ... & Mushtaq, M. (2023). An extensive study on multiple ETL and HTL layers to design and simulation of high-performance lead-free CsSnCl3-based perovskite solar cells. Scientific Reports, 13(1), 2521.

[10]. Hu, Z., Ran, C., Zhang, H., Chao, L., Chen, Y., & Huang, W. (2023). The current status and development trend of perovskite solar cells. Engineering, 21, 15-19.

[11]. Zanuccoli, M., Semenihin, I., Michallon, J., Sangiorgi, E., & Fiegna, C. (2013). Advanced electro-optical simulation of nanowire-based solar cells. Journal of Computational Electronics, 12, 572-584

[12]. Bin, H., Wang, J., Li, J., Wienk, M. M., & Janssen, R. A. (2021). Efficient Electron Transport Layer Free Small-Molecule Organic Solar Cells with Superior Device Stability. Advanced Materials, 33(14), 2008429..

[13]. Ismail, Z. S., Sawires, E. F., Amer, F. Z., & Abdellatif, S. O. (2023). Experimentally verified analytical models for the dynamic response of perovskite solar cells using measured I–V and C–V characteristics. Optical and Quantum Electronics, 55(14), 1272.

[14]. Girtan, M., Mallet, R., Socol, M., & Stanculescu, A. (2020). On the physical properties PEDOT: PSS thin films. Materials Today Communications, 22, 100735.

[15]. Ren, G., Han, W., Deng, Y., Wu, W., Li, Z., Guo, J., ... & Guo, W. (2021). Strategies of modifying spiro-OMeTAD materials for perovskite solar cells: a review. Journal of Materials Chemistry A, 9(8), 4589-4625.

[16]. Tawalbeh, M., Al-Othman, A., Kafiah, F., Abdelsalam, E., Almomani, F., & Alkasrawi, M. (2021). Environmental impacts of solar photovoltaic systems: A critical review of recent progress and future outlook. Science of The Total Environment, 759, 143528.

[17]. Zhang, S., & Sun, J. (2023). Design and optimization of ARC solar cell with intrinsic layer and p–n junction in bottom cell under AM1. 5G standard spectrum. Emergent Materials, 6(1), 159-166.

[18]. Elion, G. R. (2020). Electro-optics handbook. CRC Press.

[19]. Chen, R., Long, B., Wang, S., Liu, Y., Bai, J., Huang, S., ... & Chen, X. (2021). Efficient and stable perovskite solar cells using bathocuproine bilateral-modified perovskite layers. ACS Applied Materials & Interfaces, 13(21), 24747-24755.

[20]. Hashemi, M., Minbashi, M., Ghorashi, S. M. B., Ghobadi, A., Ehsani, M. H., Heidariramsheh, M., & Hajjiah, A. (2021). Electrical and optical characterization of sprayed In2S3 thin films as an electron transporting layer in high efficient perovskite solar cells. Solar Energy, 215, 356-366.

[21]. Asgary, S., Moghaddam, H. M., Bahari, A., & Mohammadpour, R. (2021). Role of BCP layer on nonlinear properties of perovskite solar cell. Solar Energy, 213, 383-391.

ОПТИМІЗАЦІЯ СТРУКТУРИ СОНЯЧНОЇ КОМІРКИ НА ОСНОВІ ПЕРОВСКІТУ

Н. Кузик, С. Куцій

Національний університет "Львівська політехніка", вул. С. Бандери, 12, Львів, 79013, Україна

Експериментально виготовлено перовскітну сонячну комірку (PSC) зі структурою Au/Spiro-MeOTAD/CH3NH3PbI3/PEDOT:PSS/ITO. Емпірично отримано основні фотоелектричні характеристики структури, а саме вольт-амперні характеристики (ВАХ), виміряні у діапазоні напруги від -1В до 1В. Під час вимірювань були розраховані відповідні значення густини струму короткого замикання (Jsc) 1,23 мА/см² та напруги холостого ходу (Uoc) 0,19 В відповідно. Аналітично сформована модель, що відповідає виготовленому зразку. Для моделювання параметрів гетероструктури перовскітового сонячного елемента використовувалося середовище Comsol Multiphysics, побудоване на методі скінченних елементів. Теоретично обчислено значення густини струму короткого замикання 3,29 мА/см² та напруги холостого ходу 0,2 В. Використовуючи системне забезпечення Comsol визначено максимальну потужність структури для експериментального зразка та теоретичної моделі цієї ж структури 0,11 Вт та 0,43 Вт відповідно. Співставлено результати експерименту та аналітичної моделі. Результати моделювання пройшли експериментальну верифікацію. Оптимізована аналітична модель структури була побудована шляхом додавання електронно транспортного шару (ETL). Для покращення ефективності комірки використано органічний матеріал BCP (Bathocuproine), у якості додаткового шару ETL. Теоретично обчислено ВАХ, що уможливило подальші розрахунки значення щільності струму короткого замикання 10,17 мА/см², напруги холостого ходу 1,2 В та максимального значення потужності структури Au/BCP/Spiro-MeOTAD/CH3NH3PbI3/PEDOT:PSS/ITO, що становить 3,21 В. Проведено

порівняння вольт-амперних характеристик комірок перовскіту в темновому та світлому режимах для первинної та оптимізованої структур. Заразом зроблено порівняння основних параметрів, отриманих під час моделювання експериментального зразка та подальшої оптимізованої моделі. Зокрема, було оцінено один із ключових параметрів гетероструктур сонячних елементів, коефіцієнта заповнення, який збільшився з 16,52% до 25,00% відповідно. Світлочутливі параметри перовскітноїкомірки були помітно покращені.

Ключові слова: *гетероструктира, сонячна батарея, перовскіти, органічні фотоелектричні пристрої*